# Impact of composition of extended objects on percolation on a lattice

Grzegorz Kondrat*
*Institute of Theoretical Physics, University of Wrocław, plac M. Borna 9, 50-204 Wrocław, Poland*
(Received 18 January 2008; revised manuscript received 15 May 2008; published 1 July 2008)

We consider the percolation aspect of random sequential adsorption of extended particles onto a two-dimensional lattice using computer Monte Carlo simulations. We investigate how the composition of the particles influences the value of the percolation threshold. Two regimes can be distinguished: one for almost linear particles (with the composition of straight segments reaching 85–100 %) and the second one for more bent (flexible) ones. For more bent particles we found a high correlation between the percolation threshold and the structure of an adsorbate at percolation. We also observe that there is no difference in the conclusions for both kinds of lattice considered (square and triangular).

DOI: 10.1103/PhysRevE.78.011101 PACS number(s): 64.60.ah, 61.46.Bc, 61.43.Hv

## I. INTRODUCTION

Even though the problem of percolation [1] has been known for many years [2] and many papers have dealt with its various aspects, there are still many interesting questions to be answered. In a basic lattice formulation, each site is occupied with the probability $c$ or is empty with the complementary probability $1-c$. As $c$ increases from 0, neighboring occupied sites start to form connected clusters with greater and greater size. Eventually, for a certain threshold value $c_p$, there appears an "infinite" cluster that spans the whole system. The probability threshold depends on the system's size $L$, but it has a finite limit as $L\to\infty$ (the convergence is a power law [1]). There are many applications of the percolation theory in physics and chemistry, especially in disordered systems, porous media, and critical phenomena. Percolation is the simplest nontrivial model of phase transitions and is widely used in describing transition phenomena [3] (e.g., gelation). Other important applications include resistivity of composites [4,5] and strain behavior of solids [6].

There are several mechanisms of particle deposition onto a surface, but among them random sequential adsorption (RSA) both is relatively simple and has many successful applications in theory and experiment. The starting point in this approach is usually an empty substrate surface. The process of adsorption is sequential, i.e., there is only one particle being adsorbed at a time. The position and orientation of the adsorbed particle at each trial is generated randomly. The result of each trial is determined by a nonoverlapping rule: the trial is accepted (and the particle is adsorbed) if there is no overlapping with the previously adsorbed particles. However, if any part of the particle overlaps with some other particles, the whole trial is rejected and a new position and orientation (in some models also a new shape) is generated again (without any correlation to previous trials). The whole process is irreversible—adsorbed particles stay on the surface forever at the adsorbed positions.

The RSA approach originates from the work of Flory [7], who studied a cyclization reaction in a polymer chain in which adjacent pendant groups link randomly. In general, in RSA-type models [8–13] one usually consider atoms, molecules, or geometric shapes like circles, lines, or ellipses that adsorb on polymer chains, solid surfaces, biological membranes, or lattice or continuum planes. These models are widely used in various fields of physics and chemistry, especially where one deals with irreversible processes. The approach of RSA has been used, among others, in models for reactions on polymer chains [7,14], chemisorption on crystal surfaces [15], adsorption in colloidal systems [16,17], random growth in surface physics [18], growth processes in three-dimensional (3D) solid state physics [19,20], technology of composites [21], granular matter study [22], and disordered systems [23] and also in the wider context of ecology [24] or sociology [25]. For an extensive overview of the field, see Refs. [26–28].

Recently the irreversible adsorption of large particles (polymers, nanoparticles, etc.) has attracted much attention. Among many papers devoted to the subject one can mention Ref. [29], where blocking effects in the adsorption dynamics of linear macromolecules are explored. In Ref. [30] a scale-invariant behavior of the jamming time for linear particles adsorbed on arbitrary finite square lattices is revealed. An analytical derivation of the power law describing the size of jamming fluctuations on homogeneous and inhomogeneous lattices can be found in [31]. The other shapes on a triangular lattice as well as their mixtures were considered in Ref. [32] (see also references therein), where the approach to jamming was investigated. There is an interesting comparison study of lattice adsorption versus continuous adsorption in Ref. [33].

Relatively many papers have been devoted to determining the universality class and the threshold for the percolation of particles modeled by random walks of given length; see Refs. [34–36]. Additional effects connected to nonperiodicity of the substrate (or contamination of the underlying regular lattice) were studied in Refs. [37–39]. Some generalizations of the problem using mixed side-bond percolation can be found in Refs. [40,41]. The interplay between jamming and percolation for monomers, dimers, and square particles at various temperatures was studied in Refs. [42–45]. An interesting model of percolation of very large polymers (with the length of order of the system size) is discussed in Ref [46]. Some aspects of percolation in nanocomposite films were described in Ref. [47].

*gkon@ift.uni.wroc.pl

 

The solutions of most percolation problems are of mainly approximate nature, since the exact calculations can be done only in very special cases (e.g., $c_p$ for random percolation on a triangular lattice or percolation on Bethe lattices [1]). We decided to perform Monte Carlo simulations of the problem since other approaches did not prove promising.

The paper is organized as follows. In Sec. II we describe the details of the model. A discussion of finite-size scaling and the error bars of the data is included in Sec. III. The main results of the paper are presented in Sec. IV. The reasons for lack of percolation for some sets of parameters are discussed in Sec. V. Additional data on the other (triangular) lattice confirming the previous conclusions (drawn for the square lattice in Sec. IV) are described in Sec. VI. Some additional facts on cluster structure are put forward in Sec. VII. Concluding remarks are included in Sec. VIII.

## II. MODEL

In this paper we study adsorption of extended particles of fixed length on a lattice. The coverage of the surface is increased in the process up to the percolation threshold, when there appears a so-called infinite cluster (a cluster that extends through the whole system). The resulting percolation threshold depends on the spatial structure of the particles being adsorbed and their size. We investigate here by means of Monte Carlo simulations how the composition and the size of the particles determine the threshold. Other aspects of a similar model were studied in Ref. [48]. In order to obtain a deeper insight into the problem we carried out simulations on two kinds of 2D lattice: square and triangular.

Each particle is modeled here as a group of $a$ consecutive neighboring sites (monomers) of the lattice (we deal with unbranched polymers). Between successive monomers we have bonds that form a broken line (the backbone of the particle). By the composition of the particle we understand here the fractions of corresponding bending types in a backbone. On a square lattice there are only two types of bending: straight ($S0$) and at right angles ($S1$); on a triangular lattice we have three: straight ($T0$), slightly bent at the angle of 120° ($T1$), and highly bent at the angle of 60° ($T2$); see Fig. 1. For a given particle composition ($p_0$, $p_1$) for the square lattice and ($p_0$, $p_1$, $p_2$) for the triangular one, we put particles on a lattice randomly (details below) until percolation appears. Then the resulting density of the particles is calculated (the ratio of occupied sites of the lattice to the number of all sites accessible). To obtain statistically reliable results with a low level of fluctuations we carry on the simulations for a given composition of particles for $N=100$ times. In order to acquire a comprehensive set of data for each considered particle size ($a=3,\ldots,30$), we sample the whole space of compositions with a density step from 0.2 down to 0.01.

A single run for the given composition starts with an empty substrate (a square $L\times L$ on the square lattice, a hexagon with the edge of $L$ lattice units on the triangular one, and hard wall boundary conditions adopted in both cases). The process of adsorption is random and sequential, i.e., at any time we try to put randomly (at random position and orientation) a single particle. Its shape is generated also randomly according to the probability distribution of possible bending types ($p_0{:}p_1$ for the square lattice, $p_0{:}p_1{:}p_2$ for the triangular one). Thus the exact numbers of bending of each type can vary from particle to particle, while the average composition remains constant in a single run. If the particle under consideration overlaps with the particles previously adsorbed, the whole trial is rejected. If there is no overlapping, the particle stays there forever. In each case, we then try to put on the substrate a new particle (with a new shape) at a new position with a new orientation. We repeat this procedure until the percolation cluster arises in the system (i.e., the opposite edges of the system are connected via some path of nearest neighbor sites occupied by the particles). One can consider many definitions of the overall connectivity (e.g., any opposite edges are to be connected, given opposite edges are to be connected, all opposite edges are to be connected, etc.), but asymptotically all are equivalent [49]. Here we check the connectivity between upper and lower edges of the system. It appeared that for some values of the simulation parameters we cannot observe percolation, especially for long particles and $p_2$ very close to 1. In this case particles tend to form compact, isolated islands, so the connectivity in the system is poor. Jamming in the system sets in before percolation can appear (no more particles can be added due to a lack of free space of appropriate shape). More detailed discussion of this effect is postponed to Sec. V. For reliability of the results it is important to keep finite-size effects within reasonable limits. For bigger lattices the statistical fluctuations of the threshold obtained are smaller. Also the difference between the limiting ("exact") value of the threshold (size of the lattice $L\to\infty$) and the values obtained for a given size $L$ drops down to zero with increasing $L$. Thus it is desirable to use as large latices as possible. We carry out our simulations on lattices as big as $L=1000$ for a square lattice and $L=300$ for a triangular one. Extensive discussion of finite-size effects (scaling), statistical deviations, and errors is included in the following section.

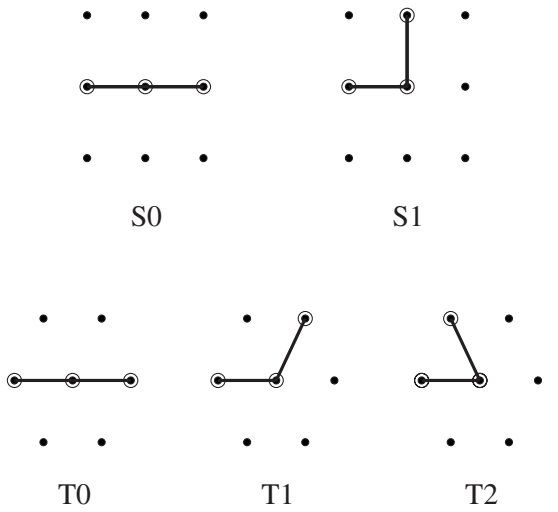


FIG. 1. Possible types of backbone bending on a square (top) and a triangular lattice (bottom).

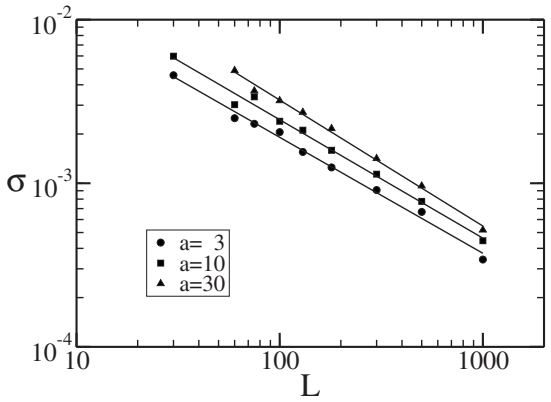


FIG. 2. Standard deviations $\sigma$ of the square lattice threshold for $a=3$, 10, and 30 as a function of the lattice size $L$. The composition parameters are $p_0=0.80$, $p_1=0.20$. Straight lines represent power law fits with exponents −0.770(21), −0.724(25), and −0.770(22) for $a=3$, 10, and 30, respectively.

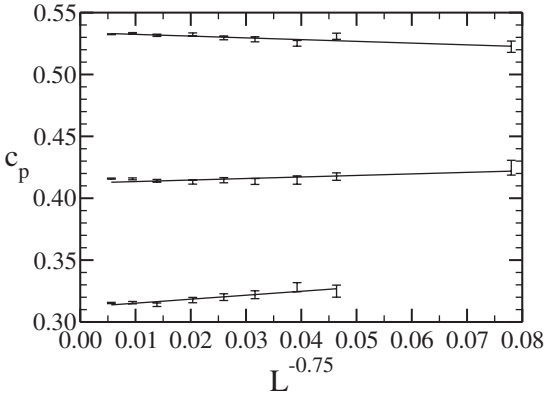


FIG. 3. Finite-size scaling of the square lattice threshold $c_p$ against $L^{-1/\nu}$ for $\nu=4/3$, particles with $a=3$, 10, and 30, and lattice size $L=30,\ldots,1000$. The composition parameters are $p_0=0.80$, $p_1=0.20$.

### III. DISCUSSION OF FINITE-SIZE SCALING

For percolation-type systems on finite lattices, it is known [1] that finite-size scaling theory describes correctly the dependence of the average threshold and its standard deviation on the size of the lattice $L$. In such systems one assumes that the probability $\Pi$ that a lattice of linear size $L$ percolates at concentration $p$ has the form $\Pi(p,L)=\Phi[(p-p^*)L^{1/\nu}]$. The scaling function $\Phi(x)$ increases from 0 to 1 as its argument $x$ increases from $-\infty$ to $+\infty$. Here $p^*$ is the infinite (exact) percolation threshold (as $L\to\infty$) and the constant $\nu$ is the critical exponent (4/3 for simple site percolation in two-dimensional systems). It appears from the scaling theory that (a) the standard deviation $\sigma$ of the threshold ($\sigma=\langle p^2\rangle-\langle p\rangle^2$) measured for a finite lattice $L$ satisfies the power law

$$\sigma \propto L^{-1/\nu}, \tag{1}$$

and (b) the effective percolation threshold $c_p$ (the mean value measured for a finite lattice) approaches the exact value $p^*$ also via power law

$$c_p - p^* \propto L^{-1/\nu}. \tag{2}$$

To check the validity of relation (1) we collected data for various sizes of the particles ($a=3,\ldots,30$), various compositions ($p_1=0,0.2,0.4,0.7,0.9$), and square lattices of various sizes ($L=30$, 60, 75, 100, 130, 180, 300, 500, and 1000). Obviously, for long particles ($a\approx 30$) we omit the lattice size $L=30$ due to extremely high finite-size effects. For all data we obtained the confirmation of Eq. (1) with the value of the exponent $1/\nu$ ranging from $0.69\pm0.02$ to $0.77\pm0.02$. This coincides with the theoretical value for two-dimensional percolation $1/\nu=0.75$. A typical log-log plot of $\sigma$ vs $L$ is given in Fig. 2. Numerical points follow the power law within reasonable accuracy.

In the following we will analyze the percolation threshold $c_p$ for $L=1000$ as a function of composition in more detail, but now we estimate the differences in the threshold value between the finite ($L=1000$) and infinite (exact) cases: $\Delta=|c_p(L=1000)-p^*|$. Plotting the mean value $c_p$ of the threshold for various lattice sizes $L$ against $L^{-1/\nu}$, we confirm the validity of the finite-size scaling in the system. From the plots we estimate the difference $\Delta\leq 0.004$ for all parameters, except for very long straight particles ($a\approx 30$ and $p_0\approx 1.00$), where $\Delta\leq 0.01$. An example of such a plot is given in Fig. 3. Our $\Delta$ stands here for the error we make taking thresholds for $L=1000$ instead of the exact ($L\to\infty$) value.

We can also ask about the statistical fluctuations and uncertainty for the chosen $L=1000$. We obtain the mean value of $c_p$ in a series of $N=100$ simulations. The statistical error of the mean is $\sqrt{N}$ times smaller than the standard deviation $\sigma$. The numerical values of this error are well below $10^{-3}$ for all parameters of the model and do not exceed $2\times10^{-4}$ for $L=1000$.

### IV. RESULTS FOR SQUARE LATTICE

In the case of the square lattice we analyzed particles of sizes between 3 and 30. We skipped the case $a<3$ (monomers and dimers), as one cannot speak about the composition of such small particles. We chose the sampling step of $p$ as 0.1, but additionally we considered a more refined grid for sufficiently small $p_1$, where the percolation threshold as a function of a composition changes more quickly (small $p_1$ implies $p_0\approx 1.0$, i.e., straight particles). The considered value of $p_1$ belongs to the set $\{0,0.01,0.02,\ldots,0,05,0.010,0.15,0.2,0.3,\ldots,1.0\}$ and the complement $p_0=1-p_1$. The percolation threshold $c_p$ is shown in Fig. 4. For all lengths and compositions of the particles we plot the resulting percolation threshold (lines are guides for the eye only), obtaining a two-dimensional surface. The sections of this surface for constant values of the length $a$ are the main point of interest in this work, since they show the composition dependence of the percolation threshold. Examples for some chosen lengths ($a=5$, 10, and 20) are shown in Fig. 5. It can be seen that the variation of composition dependence is larger for longer particles, while for the smallest ones ($a=3$) the threshold remains a nearly constant function. For all lengths, however, we observe a common qualitative behavior as $p_1$ increases from zero. For $p_1=0.0$ (thus $p_0=1-p_1=1.0$ and the particles form straight

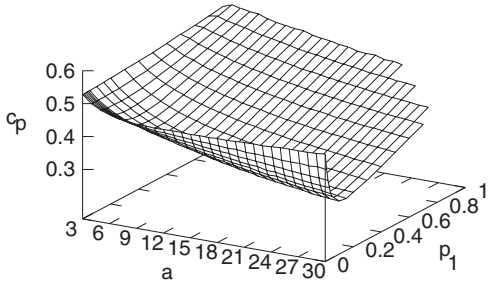


FIG. 4. Percolation threshold $c_p$ as a function of the particle size $a$ and its composition on a square lattice ($p_1$ is the relative amount of bendings of type $S1$). Here the size of the system $L=1000$. Lines are guides for the eye only.

needles) we have a local maximum; then the threshold sharply decreases as $p_1$ approaches a particular value of 0.15, for which we have a minimum. Then the function increases in a linear manner in the rest of the interval [0,1].

The fact that for higher values of $p_1$ the threshold is larger comes from the smaller diameters of such particles (to make up a percolating cluster one needs more particles, when they are more compact). In contrast, the straightest shapes (with $p_1 \approx 0.0$) do not mean the easiest way of making connections in the system (or the lowest value of the percolation threshold). This is because needlelike particles in the process of adsorption make domains of common alignment. When a linear particle is adsorbed close to another particle with the same orientation, they will be likely connected by other parallel particles. The density of a system composed of such domains is higher than for more flexible (bent) particles, where the particles have more possibilities of touching each other and the clusters have a sparser structure. It should be noticed that the changes of the threshold $c_p$ are large in the vicinity of $p_1=0$. From the experimental point of view, this means that the system is very sensitive to small deviations from linearity of the particles (in the case of less straight particles, variation of their composition results in smaller changes of the percolation threshold).

With the two above-mentioned mechanisms of increasing the threshold for either small or large values of the parameter $p_1$, one expects a minimum at some intermediate value of $p_1$.

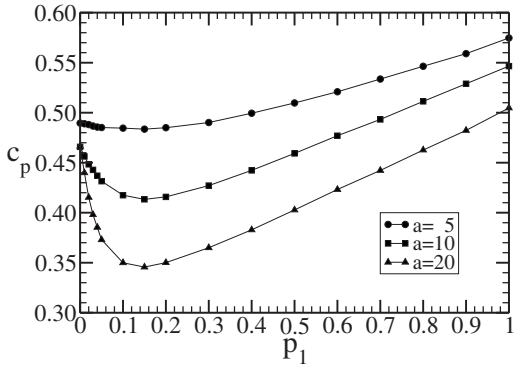


FIG. 5. Percolation threshold as a function of the particles' composition only. Each line represents a section of the surface of Fig. 4 for the given particle length (here $a=5$, 10, and 20). The size of the system $L=1000$. Lines are guides for the eye only.

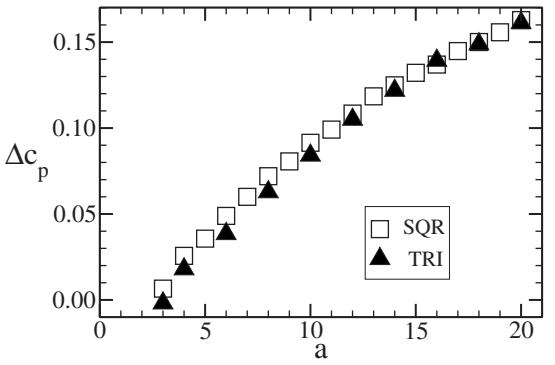


FIG. 6. Comparison of the relative height $\Delta c_p$ of the maximum of the percolation threshold for linear particles as a function of the particle length $a$ for two kinds of lattice: square (squares) and triangular (triangles). This height is measured against the reference level; see text for details. Uncertainties are smaller than the size of the symbols.

The localization of this minimum can in general depend on the size of the particles. We found, however, that it is not the case here—the value of $p_1=0.15$ is universal for particles of all sizes. That means that this specific composition ($p_0=0.85, p_1=0.15$) is the most favorable one for percolation on a square lattice. Unfortunately, a theoretical determination of that value is difficult and still needs further investigation.

We consider now the threshold $c_p(p_0,p_1)$ as a sum of a linear part (the main component) and a function with a peak around $p_1=0$ (the domain component). In particular, we measure the height of the peak of the latter in the following way. We take the difference $\Delta c_p$ between the value of $c_p$ obtained in simulations for $p_1=0$ and the linear dependence extrapolated to $p_1=0$ (we draw an extrapolation line through two points for $p_1=0.4$ and 0.7, since in that interval we have very well-pronounced linear behavior of $c_p$). The resulting height of the peak accounting for domains of parallel alignment is presented in Fig. 6. The results for the square lattice are plotted as squares. The triangles on the plot correspond to a similarly defined $\Delta c_p$ on a triangular lattice; see the detailed discussion in Sec. VI. The uncertainties of the data shown are smaller than the size of the symbols.

## V. NO-PERCOLATION REGIME

For large values of $p_1 \geq 0.8$ and for long particles ($a > 23$) there are problems in reaching percolation. For such compositions the particles are quite compact and connectivity between them is rather low. The interparticle space is narrow, so it is difficult to adsorb another big compact particle. Owing to the statistical algorithm used for generating the shape of the particles (each next bond is chosen according to probability), it is often possible to fill such a narrow-shaped space with a big particle; however, one needs an extremely large number of trials (very long expected values of adsorption times). In order to avoid waiting for practically infinite time to end a simulation, we introduced in our computer code a maximum number of allowed unsuccessful adsorption trials in a row. After reaching this limit a current run is qualified as "no-percolation" case and stopped. In Fig. 4

only such sets of parameters are taken into account, for which in all $N=100$ runs percolation was reached. For each series of simulations we introduce the quantity $N^{\mathrm{NOP}}$, the ratio of the number of no-percolation cases to all cases in a series ($N$). For $L=1000$ we obtained $N^{\mathrm{NOP}}>0$ for $a=30$ ($p_1=0.8$), $a>26$ ($p_1=0.9$), and $a>23$ ($p_1=1.0$). The finite-size scaling of $N^{\mathrm{NOP}}$ done for $L=30,\ldots,1000$ divided the considered set of parameters ($a$, $p_0$, and $p_1$) into two categories: (a) those for which $N^{\mathrm{NOP}}\to 0.0$ as $L$ increases, and (b) those for which $N^{\mathrm{NOP}}\to 1.0$ as $L$ increases. In other words, the transient set of parameters for which neither $N^{\mathrm{NOP}}\neq 0$ nor $N^{\mathrm{NOP}}\neq 1$ is shrinking as we go to larger lattices. Thus the no-percolation characteristics can be attributed to the given particles' parameters (namely, their size and composition) rather than stemming from computational limitations and finite-size effects. A similar absence of percolation in adsorption models was reported in the study of adsorption of big squares on a lattice [50,51], where no percolation was found for the size of the squares $a>3$.

## VI. RESULTS FOR TRIANGULAR LATTICE

We carried out the simulations also on the triangular lattice in order to check the universality of the studied dependencies. Indeed, the whole behavior is confirmed. The details of the triangular version of the simulations do not differ distinctly from the square case. Here we considered particles of size $a=3,\ldots,20$ and the substrate size $L$ as large as 300. These values are smaller than those for the square case mainly due to the much larger computational costs of simulations on the triangular lattice. For example, the time for$N=100$ simulations for $(p_0,p_1)=(0.2,0.8)$ and $L=300$ was about 31 000 s (nearly 9 h), while for $(p_0,p_1,p_2)=(0.2,0.4,0.4)$ and the same values of $L$ and $N$ the simulations on the triangular lattice lasted 81 000 s (22.5 h).

The typical landscape of dependence of the percolation threshold on the composition is given in Fig. 7, where $c_p$ is plotted against $p_1$ and $p_2$ (probabilities of bending types $T1$ and $T2$ of Fig. 1, respectively) for particles of size $a=10$. The three vertices of the plot, left, right, and rear, correspond to straight linear particles ($p_0=1$, $p_1=0$, and $p_2=0$), particles with bonds of type $T1$ ($p_0=0$, $p_1=1$, and $p_2=0$), and most bent particles with bonds of type $T2$ ($p_0=0$, $p_1=0$, and $p_2=1$), respectively. The arrows on the plot point to isolines of constant level of $p_1$ or $p_2$. It can be clearly seen that the behavior of the threshold is dominated by the linear part (flat surface), above which there is a peak around the leftmost vertex that corresponds to the linear straight particles.

Finite-size scaling was checked also for these data and we obtain confirmation of Eq. (1) with the value of the exponent $1/\nu$ ranging from 0.68 to 0.81 with errors $\leq 0.05$. Again this coincides with the theoretical value for two-dimensional percolation, $1/\nu=0.75$. As before, we estimate the difference in the threshold value between the finite ($L=300$) and infinite (exact) cases: $\Delta=|c_p(L=300)-p^*|$. From the plots of the mean value $c_p$ of the threshold against $L^{-1/\nu}$, we obtained the difference $\Delta\leq 0.004$ for all parameters, except for long straight particles ($a=20$ and $p_0\approx 1.00$), where $\Delta\leq 0.012$. Again the value of $\Delta$ is considered as giving the accuracy of Fig. 7.

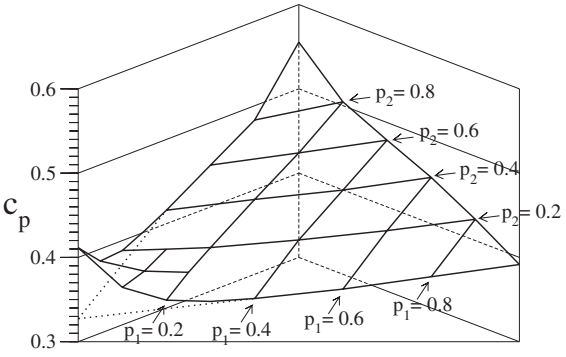


FIG. 7. Percolation threshold $c_p$ on the triangular lattice for particles of length $a=10$ as a function of their composition $(p_1,p_2)$. The arrows point to isolines of constant level of $p_1$ or $p_2$. The leftmost vertex (with $c_p\approx 0.41$) corresponds to strictly linear particles $(p_0,p_1,p_2)=(1,0,0)$; the rightmost one with $c_p\approx 0.39$ corresponds to particles made of $T1$-type bending only [composition (0,1,0)] while the rear one describes the most compact case of $c_p\approx 0.55$ and composition (0,0,1). The dotted lines approaching the value $c_p\approx 0.33$ represent the reference level, from which the height $\Delta c_p$ of the peak is measured (see more details in the text).

We now determine the height of the peak rising above the plane of Fig. 7, as it is a measure of deviation from linear behavior for straight particles. We took three representative points on the flat (linear) part of the plot, $(p_0,p_1,p_2)=(0.6,0.4,0.0)$, (0.6,0.0,0.4), and (0.2,0.4,0.4), and we extrapolate this plane to the composition of linear particles (1.0,0.0,0.0) (see the dotted lines on Fig. 7). The height of that peak, $\Delta c_p$, is plotted on Fig. 6 with triangles. One can see that the data for square and triangular lattices coincide. Here the error bars do not exceed the size of the symbols.

The most favorable composition (for which the percolation threshold acquires its minimal value) is located for all particle sizes at $p_2=0$ and $p_1$ between 0.2 and 0.3 (thus $p_0$ lies between 0.7 and 0.8). The more exact estimation of that point needs further study, however.

On the triangular lattice there are also simulations where no percolation was reached (see more detailed discussion of this effect in Sec. V). For relatively small particles ($a<14$), we arrive at percolation at every run for all compositions $(p_0,p_1,p_2)$. When we consider larger particles, more bent shapes cease to percolate while straight ones still form percolating clusters. Here the value of the percentage $p_2$ of most bent segments is crucial. For example, percolating particles for the most bent shape $(p_0=0,p_1=0,p_2=1)$ have the maximum size $a=13$, for lower $p_2$ $(p_0=0,p_1=0.4,p_2=0.6)$ the maximum size is $a=22$, but for $p_2=0$ all considered particles (up to $a=30$) percolate. The exact finite-size scaling of $N^{\mathrm{NOP}}$ in the triangular case was not done, however, due to very long times of simulations for high values of lattice size $L$ and particle size $a$.

## VII. CLUSTER STRUCTURE ANALYSIS

In order to verify the possibility of correlation between the percolation threshold and some single-particle characteristics, we checked also how the composition of the particles

affects the mean square radius of gyration and the mean end-to-end distance. It turned out that there is no sharp transition for any composition of a single particle, so the appearance of different regimes of percolation (high value of the threshold for almost straight particles, no percolation for very compact particles, mild linear dependence for the other cases) can be attributed only to collective interaction of the particles.

On the other hand, the composition of the particles influences the structure of the percolating cluster. We investigated this relation further and looked at the percentage of sites having a given number of neighbors. We found a strong correlation between the relative number of sites with exactly two neighbors (for the square lattice) and the percolation threshold. For the linear part (away from the peak for $p_0 \geq 0.8$ and no-percolation regime) the equation $c_p = 0.897(1 - R_2)$ is satisfied within an accuracy of 0.03. The quantity $R_2$ is defined as the mean ratio of a number of adsorbed sites with exactly two neighbors to the total adsorbed number of sites (monomers of the particles) at percolation, averaged over $N$ simulation runs. The collected data (for $p_0 \in [0.1, 0.8]$ in the square case) as well as the linear relation postulated above are presented in Fig. 8. The statistical errors of the points are of order $\sigma(R_2) \leq 0.02$ and $\sigma(c_p) \leq 0.015$. All data presented in Fig. 8 are obtained for lattice size $L = 300$.

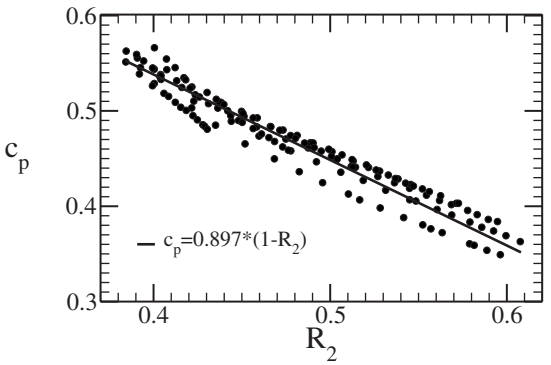


FIG. 8. Correlation between the percolation threshold $c_p$ and the percentage $R_2$ of monomers with exactly two nearest neighbors at percolation for various compositions ($p_1 = 0.2, \ldots, 0.9$) and sizes ($a = 3, \ldots, 20$) of the particles (for the square lattice). The line $c_p = 0.897(1 - R_2)$ is also shown. Statistical errors are smaller than 0.015 for $c_p$ and smaller than 0.02 for $R_2$.

## VIII. CONCLUSIONS

We analyzed the random sequential adsorption of extended particles with a given size and composition of the shape on square and triangular lattices. The shape variables on the square lattice $p_0, p_1$ (defined as the percentage of a given kind of bending in a chain) influence the percolation threshold $c_p$ in such a way that one can look at the whole landscape of the function $c_p(p_0, p_1)$ as a sum of a mildly linear part for $p_1 \geq 0.4$ and sharp peak around $p_1 = 0$. The overall behavior of the threshold $c_p$ is common on both lattices considered. In particular, the height of the peak as a function of the particle size coincides for both cases.

A linear correlation between the percolation threshold and cluster structure (more precisely, the relative amount of monomers with exactly two neighbors at percolation) was observed for particles with $0.2 \leq p_1 \leq 0.9$ (on a square lattice).

[1] D. Stauffer and A. Aharony, *Introduction to Percolation Theory* (Taylor & Francis, London, 1994).
[2] S. R. Broadbent and J. M. Hammersley, Proc. Cambridge Philos. Soc. **53**, 629 (1957).
[3] M. B. Isichenko, Rev. Mod. Phys. **64**, 961 (1992).
[4] F. Carmona, P. Prudhon, and F. Barreau, Solid State Commun. **51**, 255 (1984).
[5] A. Bunde, W. Dieterich, and E. Roman, Phys. Rev. Lett. **55**, 5 (1985).
[6] P. C. Robinson, J. Phys. A **16**, 605 (1983).
[7] P. J. Flory, J. Am. Chem. Soc. **61**, 1518 (1939).
[8] M. D. Khandkar, A. V. Limaye, and S. B. Ogale, Phys. Rev. Lett. **84**, 570 (2000).
[9] R. S. Ghaskadvi and M. Dennin, Phys. Rev. E **61**, 1232 (2000).
[10] B. Bonnier, Phys. Rev. E **54**, 974 (1996).
[11] J.-S. Wang and R. B. Pandey, Phys. Rev. Lett. **77**, 1773 (1996).
[12] A. Matsuyama, R. Kishimoto, and T. Kato, J. Chem. Phys. **106**, 6744 (1997).
[13] C. K. Gan and J.-S. Wang, J. Chem. Phys. **108**, 3010 (1998).
[14] A. C. Balazs and I. R. Epstein, Biopolymers **23**, 1249 (1984).
[15] A. Cordoba and J. J. Luque, Phys. Rev. B **31**, 8111 (1985).
[16] V. Privman, H. L. Frish, N. Ryde, and E. Matijvec, J. Chem. Soc., Faraday Trans. **87**, 1371 (1991).
[17] Z. Adamczyk, T. Babros, J. Czarnecki, and T. G. M. van de Ven, Adv. Colloid Interface Sci. **19**, 183 (1983).
[18] L. Finegold and J. T. Donnell, Nature (London) **278**, 443 (1979).
[19] J. W. Evans, D. E. Sanders, P. A. Thiel, and A. E. DePristo, Phys. Rev. B **41**, 5410 (1990).
[20] J. Fransaer, Ph.D. thesis, Katholieke Universiteit Leuven, 1994.
[21] N. Provatas, M. Haataja, E. Seppälä, S. Majaniemi, J. Åström, M. Alava, and T. Ala-Nissila, J. Stat. Phys. **87**, 385 (1997).
[22] K. Trojan and M. Ausloos, Physica A **351**, 332 (2005).
[23] L. Zhang and P. R. Van Tassel, J. Chem. Phys. **112**, 3006 (2000).
[24] M. Hasegawa and M. Tanemura, in *Recent Developements in Statistical Inference and Data Analysis*, edited by K. Matusita (North-Holland, Amsterdam, 1980).
[25] Y. Itoh, J. Appl. Probab. **17**, 134 (1980).
[26] N. Provatas, M. Haataja, J. Asikainen, S. Majaniemi, M. Alva, and T. Ala-Nissila, Colloids Surf., A **165**, 209 (2000).
[27] J. W. Evans, Rev. Mod. Phys. **65**, 1281 (1993).
[28] J. Talbot, G. Tarjus, P. R. Van Tassel, and P. Viot, Colloids Surf., A **165**, 287 (2000).
[29] P. B. Shelke, A. G. Banpurkar, S. B. Ogale, and A. V. Limaye,

Surf. Sci. **601**, 274 (2007).
[30] A. E. Bea, I. M. Irurzun, and E. E. Mola, Phys. Rev. E **73**, 051604 (2006).
[31] E. S. Loscar, R. A. Borzi, and E. V. Albano, Phys. Rev. E **68**, 041106 (2003).
[32] I. Lončarević, Lj. Budinski-Petković, and S. B. Vrhovac, Eur. Phys. J. E **24**, 19 (2007).
[33] A. Cadilhe, N. A. M. Araújo, and V. Privman, J. Phys.: Condens. Matter **19**, 065124 (2007).
[34] Y. Wu, B. Schmittmann, and R. K. P. Zia, J. Phys. A **41**, 025004 (2008).
[35] V. Cornette, A. J. Ramirez-Pastor, and F. Nieto, Physica A **327**, 71 (2003).
[36] V. Cornette, A. J. Ramirez-Pastor, and F. Nieto, Eur. Phys. J. B **36**, 391 (2003).
[37] G. Kondrat, J. Chem. Phys. **122**, 184718 (2005).
[38] G. Kondrat, J. Chem. Phys. **124**, 054713 (2006).
[39] V. Cornette, A. J. Ramirez-Pastor, and F. Nieto, J. Chem. Phys. **125**, 204702 (2006).
[40] M. Dolz, F. Nieto, and A. J. Ramirez-Pastor, Eur. Phys. J. B **43**, 363 (2005).
[41] M. Quintana, I. Kornhauser, R. López, A. J. Ramirez-Pastor, and G. Zgrablich, Physica A **361**, 195 (2006).
[42] F. Rampf and E. V. Albano, Phys. Rev. E **66**, 061106 (2002).
[43] E. S. Loscar, R. A. Borzi, and E. V. Albano, Phys. Rev. E **74**, 051601 (2006).
[44] M. C. Gimenez, F. Nieto, and A. J. Ramirez-Pastor, J. Chem. Phys. **125**, 184707 (2006).
[45] N. I. Lebovka, N. V. Vygornitskii, and A. V. Palikhov, J. Mol. Liq. **127**, 93 (2006).
[46] M. Gopalakrishnan, B. Schmittman, and R. K. P. Zia, J. Phys. A **37**, L337 (2004).
[47] T. K. H. Starke, C. Johnston, and P. S. Grant, Scr. Mater. **56**, 425 (2007).
[48] G. Kondrat, J. Chem. Phys. **117**, 6662 (2002).
[49] F. Yonezawa, S. Sakamoto, and M. Hori, Phys. Rev. B **40**, 636 (1989).
[50] M. Nakamura, Phys. Rev. A **36**, 2384 (1987).
[51] M. Porto and H. E. Roman, Phys. Rev. E **62**, 100 (2000).